Nonradiative energy transfer from high-lying highly-quenched multiplets of Nd^{3+} in the LaF_3 laser crystal

T. T. Basiev and Yu. V. Orlovskiĭ

Institute of General Physics, Academy of Sciences of the USSR
(Submitted 13 June 1989)
Zh. Eksp. Teor. Fiz. **96**, 1965–1983 (December 1989)

Direct nanosecond laser excitation and direct detection of luminescence by single-photon counting with a time resolution of 0.3 ns was used in the first experimental investigation of the nanosecond kinetics of nonradiative relaxation of highly-quenched levels of Nd^{3+} for different concentrations of this ion in the LaF_3 laser crystal. The concentration dependence of luminescence decay was investigated for the $^4G_{7/2}$ level to identify the static Förster dipole-dipole mechanism of concentration quenching with an anomalously high energy transfer microparameter, which was found to be $C_{DA} = 3.3 \cdot 10^{-37}$ cm^6/s (greater by four orders of magnitude than for the $^4F_{3/2}$ level of Nd^{3+} in LaF_3). It is shown that concentration quenching of the $^4G_{7/2}$ level via the $^4G_{7/2} \rightarrow {}^4G_{5/2} + {}^2G_{7/2}$, $^4I_{9/2} \rightarrow {}^4I_{11/2}$, cross-correlation infrared channel can be more effective (by two or three orders of magnitude) then via the high-frequency $^4G_{7/2} \rightarrow {}^4I_{11/2}$, $^4I_{9/2} \rightarrow {}^4G_{5/2} + {}^2G_{7/2}$ channel. The transfer microparameter C_{DA} has been determined at $T = 77$ and 300 K for the Nd^{3+} ion in the LaF_3 crystal on the assumption of the dipole-dipole Förster quenching, using the energy transfer kinetics for each of the $^4D_{3/2}$, $^2P_{3/2}$ and $^4G_{5/2} + {}^2G_{7/2}$ levels. Values obtained in this way are in reasonable agreement with the overlap between the luminescence spectra due to each of these multiplets and the $^4I_{9/2} \rightarrow {}^4I_{11/2}$ and $^4I_{9/2} \rightarrow {}^4I_{13/2}$ infrared absorption spectra.

The nonradiative transfer of electronic excitation energy in concentration laser crystals is one of the fundamental problems in solid state physics and quantum electrodynamics, and is of considerable applied interest. For example, the concentration quenching of luminescence emitted in transitions from the upper working laser level produces a reduction in the quantum yield and a lifting of the generation threshold. When a lamp is used as a broad-band pump, generation is preceeded by redistribution of energy between the working levels, and this can lead to a substantial change in the generation efficiency. There is particular interest in the analysis of the nonradiative transfer of energy from high-lying highly-depleted levels in Nd^{3+} activated laser crystals because cross-relaxations can give rise to transitions from these states not only to the $^4F_{3/2}$ metastable working level, but also to lower-lying laser levels. Moreover, a Stokes or anti-Stokes pump[1] can be used, at least in principle, to produce generation from high-lying levels, and this has stimulated interest in the mechanism responsible for concentration quenching of such levels.

Until now, studies of the nonradiative transfer of energy between rare-earth ions have been confined to the microsecond and millisecond time ranges[2–4] because of the low efficiency of this transfer from the metastable state. However, it has been shown[5] that, for low concentrations of the Nd^{3+} ions in fluoride laser crystals, the intracenter decay of highly-quenched high-lying levels occurs mostly (and exponentially) in the radiationless channel in a time of 5–110 ns. We have used this experimental technique to measure the concentration dependence of the quenching of luminescence from the $^4G_{7/2}$ level of Nd^{3+} in LaF_3 crystals pumped directly by laser pulses.

Figure 1 shows the quenching of luminescence from the $^4G_{7/2}$ level of Nd^{3+} for different concentrations ($c = 0.1$–24.4%) at $T = 77$ K. For samples with $c = 2.3$ and 11.3%, the relative concentration of the Nd^{3+} ions was determined by local microprobe x-ray analysis, using the Camebax system. The relative concentration of Nd^{3+} ions in the other samples was determined from the total area under the absorption spectra due to the $^4I_{9/2} \rightarrow {}^4G_{9/2}$ and $^4I_{9/2} \rightarrow {}^4G_{7/2}$ transitions, recorded with the SS-20 spectrophotometer in arbitron transmission units. These data were then converted to values of the absorption coefficient k in cm^{-1} (after calibration against the area of the analogous optical spectrum with $c = 11.3\%$, assuming that the optical transition probabilities and cross sections were constant along this series of crystals). Figure 1 shows that, as the concentration of the Nd^{3+} ions increases, the decay process is accelerated and becomes less exponential. This suggests strong anomalous concentration quenching of luminescence from the $^4G_{7/2}$ level which, in contrast to the quenching of the $^4F_{3/2}$ metastable level,[2] was observed on the nanosecond time scale.

In the general case of concentration-quenched luminescence, the nonexponential decay of donor states is well described by the following expression[6]:

$$I_L(t) = I_0 \exp[-t/\tau - P(t) - \overline{W}t], \quad (1)$$

where $1/\tau$ is the probability of intracenter decay, $P(t)$ describes the kinetics of nonradiative energy transfer in the absence of energy migration over the donors, and $\overline{W}$ is the nonradiative decay constant due to the migration of energy over donors to acceptors. In the dipole-dipole interaction between a donor and a donor, and a donor and an acceptor, the diffusion model of migration[4,7] predicts that

$$\overline{W} = 0.68 \cdot 4\pi n_A n_D \alpha^{3/4} C_{DD}^{3/4} C_{DA}^{1/4}, \quad (2)$$

where n_A is the acceptor concentration, n_D is the donor concentration, $C_{DD} = W_{DD} R^6$ is the microefficiency of the donor-donor migrational transfer of energy, W_{DD} is the proba-

 0038-5646/89/121109-10$04.00

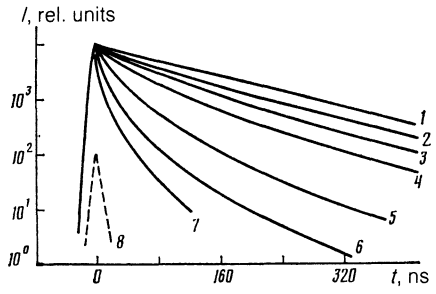

FIG. 1. Decay of luminescence from the $^4G_{7/2}$ level of Nd^{3+} in the LaF_3 crystal for λ_{exc} nm, $\lambda_{reg} = 522$ nm, and different concentrations (*1*—$c = 0.1\%$, *2*—1%, *3*—2.3%, *4*—4.7%, *5*—11.3%, *6*—16.8%, *7*—24.4%, *8*—laser pump pulse) at $T = 77$ K.

bility of migration in a pair of ions at a distance R, $C_{DA} = W_{DA}R^6$ is the microefficiency of the donor-acceptor quenching transfer, W_{DA} is the probability of quenching in a pair, and α is a numerical coefficient that is different in different theoretical models, and its measured value is[4] 1.9 ± 0.2.

For the "hopping" model of migration-controlled quenching and the dipole-dipole interaction,[8]

$$\overline{W} = \pi\,(^2/_3\pi)^{5/3} C_{DA}^{1/2} C_{DD}^{1/2} n_A n_D. \tag{3}$$

For the dipole-dipole interaction, the limiting conditions for the validity of these two migration models of quenching are as follows.[4] In the case of diffusion

$$(C_{DA}/C_{DD})^{1/2} \gg 1, \tag{4}$$

whereas in the case of the hopping model

$$(C_{DA}/C_{DD})^{1/2} \leqslant 1. \tag{5}$$

In the first approximation, the experimental data on radiationless transfer kinetics were analyzed in terms of the theory of static energy transfer, due to the multipole interaction between ions, for which electronic excitation prior to emission or quenching remains unaffected.[9,10] The quantity $\overline{W}$ in (1) is then equal to zero, and the nonradiative transfer kinetics is reasonably described by a two-stage process. During the initial stage, i.e., the so-called ordered stage, decay proceeds with maximum possible rate for a given activator and is described by the simple exponential law[10]

$$I_n(t) = I_0 \exp\left[-C_{DA} c_A \left(\sum_n 1/R_n^s\right) t\right] = I_0 \exp(-W_0 t), \tag{6}$$

where the quenching rate is given by

$$W_0 = c_A C_{DA} \sum_n R_n^{-s}, \tag{7}$$

and the sum is evaluated over all the sites of the acceptor sublattice, taking into account its population $c_A = n_A/n_{max}$. The acceptors can be the unexcited Nd^{3+} ions whose concentration is much greater than the concentration of excited ions, i.e., $n_A = n(Nd^{3+})$, and $S = 6$ for the dipole-dipole interaction, $S = 8$ for the dipole-quadrupole interaction, $S = 10$ for the quadrupole-quadrupole interaction, and so on.

From a certain instant t_1 onward, the ordered stage goes over to the so-called disordered or first Förster stage, which is reasonably well described by[9,4]

$$I_n(t) = \exp(-\gamma t^{3/S}), \tag{8}$$

where

$$\gamma = {}^4/_3\pi\Gamma(1-3/S) C_{DA}^{3/S} n_A, \tag{9}$$

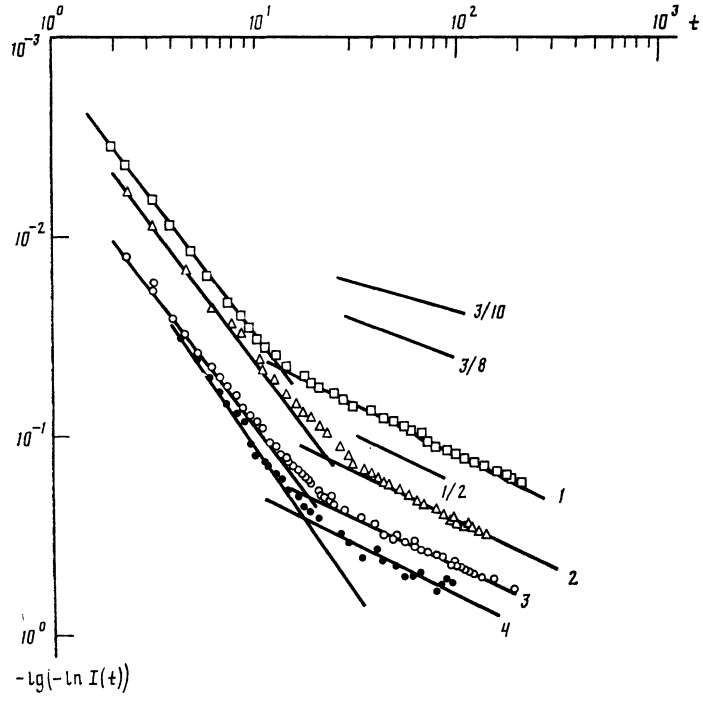

FIG. 2. Nonradiative energy transfer from the $^4G_{7/2}$ level of Nd^{3+} for different concentrations in the LaF_3 crystal: *1*—$c = 4.7\%$, *2*—11.3%, *3*—16.8%, *4*—24.4% at $T = 77$ K.

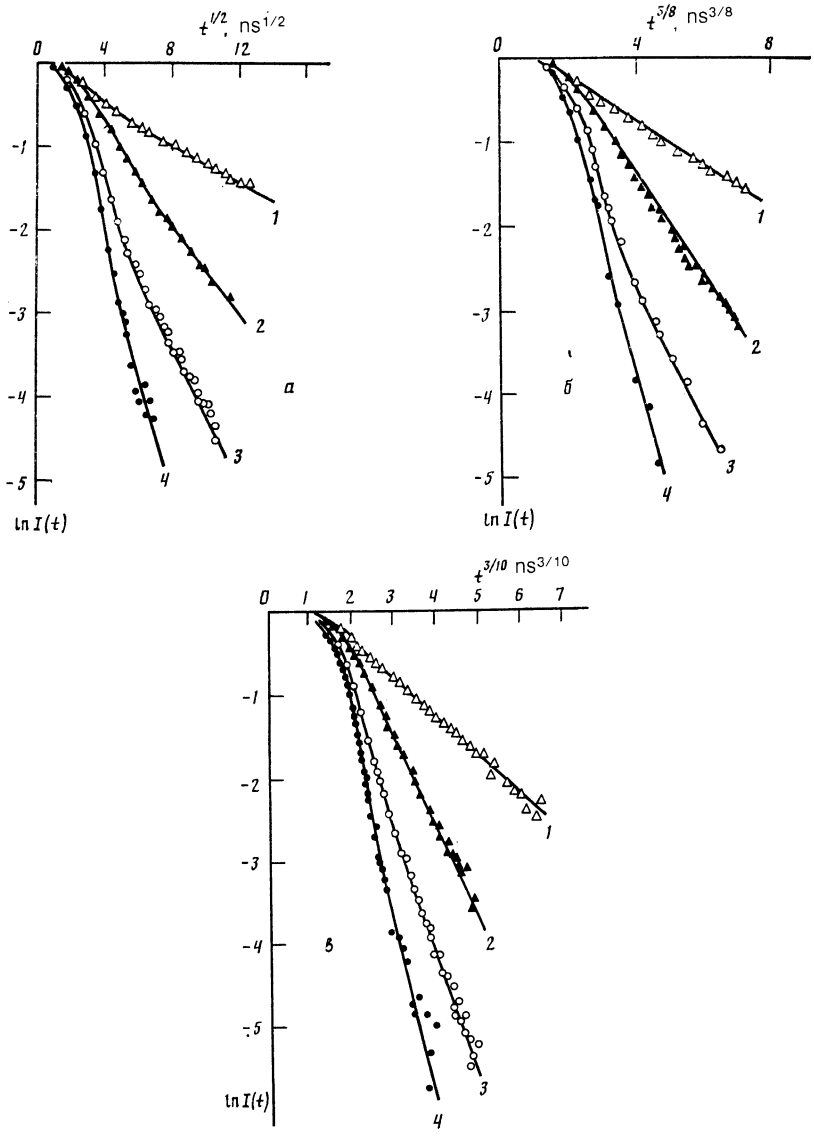

FIG. 3. Nonradiative energy transfer from the $^4G_{7/2}$ level of Nd^{3+} for different concentrations in the LaF_3 crystal: ln $I(t)$ as a function of $t^{1/2}$(*a*), $t^{3/8}$ (b), and $t^{3/10}$ (c) at $T = 77$ K (*1*—$c = 4.7\%$, *2*—11.3%, *3*—18.8%, *4*—24.4%).

and $\Gamma(x)$ is the gamma-function.

These expressions were derived by integration, assuming a continuous medium and neglecting the particle sizes or the crystal lattice constant ($R_{\min} \to 0$).

Experimental data on the luminescence decay kinetics can be analyzed in terms of the model (6)–(9) by plotting in terms of the coordinates $[-\lg(-\ln I(t))]$ and $[\lg t]$ (Fig. 2).

The slope of these graphs gives the exponent of the time parameter, which enables us to distinguish the ordered stage with $\operatorname{tg}\varphi = 1$ [see (6)] from the disordered stage with $\operatorname{tg}\varphi = 3/S$ [see (8)], and to determine S for the latter. We found that $\operatorname{tg}\varphi$ eventually tends to 1/2, which corresponds to $S = 6$ and suggests the dipole-dipole quenching interaction for the Nd^{3+} ions. If we use the coordinates ln $I(t)$ and $t^{1/2}, t^{3/8}, t^{3/10}$ (Fig. 3), these graphs can be linearized, which means that S cannot be determined from Fig. 3 alone, but the slope can be used to determine the macroparameter γ for all concentrations of the Nd^{3+} ion and any of the above three values of S. Figure 4 shows γ as a function of the concentration of Nd^{3+} ions for $S = 6$, 8, 10. It is clear that the linear law (9) is best satisfied for $S = 6$, but the fit is not as good as for $S = 6$ and 10. This confirms the dipole-dipole type of the Nd–Nd quenching interaction.

The values of the macroparameter γ obtained by ana-

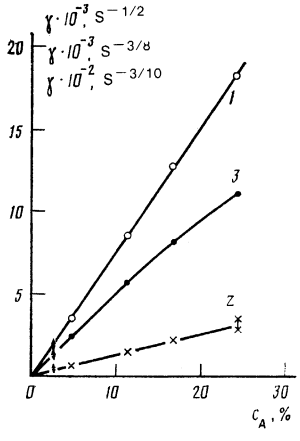

FIG. 4. Concentration dependence of the transfer microparameter γ for $S = 6$ (curve 1), $S = 8$ (curve 2), and $S = 10$ (curve 3) for the $^4G_{7/2}$ level of Nd^{3+} in the LaF_3 crystal at $T = 77$ K; $c_A = n_A/n_{\max}$.

lyzing the disordered stage are listed in the Table. The values of the quenching microparameter C_{DA} (at $T = 77$ K) for the $^4G_{7/2}$ level and the disordered stage, determined from the slope of the decay curves (Fig. 3) for $S = 6$, 8, and 10, are 3.3×10^{-37}, 4.0×10^{-51}, and 4.2×10^{-65} cm^6/s, respectively. For $S = 6$, the quantity C_{DA} was found to be unusually high and to exceed by four orders of magnitude the quenching microparameter for the metastable level $^4F_{3/2}$ of the Nd^{3+} ion (cf., for example, Ref. 2) ($C_{DA}^{^4F_{3/2}} = 1.3\times10^{-41}$ cm^6/s and $C_{DA}^{^4G_{7/2}} = 3.3\times10^{-37}$ cm^6/s). As the temperature is raised from 77 to 300 K, the value of the transfer microparameter C_{DA} for the $^4G_{7/2}$ level of the Nd^{3+} ion in the $^4F_{3/2}$ crystal falls by a factor of 1.4 an settles down to the value of 2.4×10^{-37} cm^6/s, whereas for the $^4F_{3/2}$ level it increases by a factor of 2.3 ($C_{DA}(300) = 3\times10^{-41}$ cm^6/s), i.e., the temperature dependence is basically different. To verify this value of the transfer microparameter C_{DA} and the value of S by some other independent method, e.g., for the initial ordered stage of luminescence decay [(6) and (7)], we must know the lattice sum $\Sigma_n 1/R_n^S$ for the lanthanum sublattice of the LaF_3 crystal. The structure of the unit cell of this crystal is well-known.[11] It has hexagonal symmetry, the same translation vector $a = 7.19$ Å along the x and y axes, and a different translation vector along the z axis $c = 7.367$ Å. The lattice constants of LaF_3 and NdF_3 differ by approximately 2.3%, but this was ignored in our calculations. The lattice sums were computed by confining our attention to 120 coordinate spheres of the lanthanum sublattice, i.e., 740 Nd^{3+} ions. For $S = 6$, we found that

$$\sum_n 1/R_n^6 = 2.4\cdot10^{45}\ \text{cm}^{-6},$$

which differs from the analogous value reported in Ref. 2 (8×10^{45} cm^{-6}).

To verify the convergence of the problem, we calculated the total lattice sum by a different method. A precise calculation was made of the lattice sum for the first two coordination spheres of the ion La^{3+} ($R_{\text{sph }1} = 4.151$ Å and $R_{\text{sph }2} = 4.395$ Å) in the lanthanum sublattice of the LaF_3 crystal ($\Sigma_n R_n^{-6} = 2.013\times10^{45}$ cm^{-6}); for the remaining ions, the summation was replaced by integration, bearing in mind the maximum possible concentration of the ND^{3+} ions that replace the La^{3+} ions. The replacement of the sum by the integral was made as follows:

$$\sum_n R_n^{-6} = n_{max}\int_{R_{\text{sph }3}}^{\infty} 4\pi R^2\frac{dR}{R^6}, \qquad (10)$$

where $n_{\max} = 1.76\times10^{22}$ cm^{-3} and $R_{\text{sph }3} = 6.045$ Å.

The integral (10) was found to be equal to 0.335×10^{45} cm^{-6}. By adding the values obtained for the two spheres and the integral, we find that the lattice sum is 2.35×10^{45} cm^{-6}, which is in good agreement with the value computed for 740 ions. For $S = 8$, the lattice sum was found to be 1.18×10^{60} cm^{-8} and for $S = 10$ it was 6.34×10^{74} cm^{-10}. Once we know the concentration C_A of the Nd^{3+} ions, the number of ions in each coordinate sphere, and their radii in the lanthanum sublattice of LaF_3, we can simulate on a computer the radiationless static decay in accordance with the well-known expression[10]

$$I_n(t) = \exp\Big[\sum_n \ln(1-c_A+c_A\exp(-W_{DA}(R_n)t))\Big], \qquad (11)$$

which accurately describes energy transfer in an ensemble of donors and acceptors for any value of S, without using any of the assumptions admitted in the derivation of (8) and (9). The expression given by (6) for the ordered stage can be deduced from (11) by assuming that $tW_{DA}\to0$. On the other hand, if we replace the summation in (11) with integration, and assume that $R_{\min}\to0$, we obtain the expression for the disordered Förster stage [cf. (8) and (9)].

Figure 5 shows the experimental data on nonradiative transfer (solid lines) in the case of the $^4G_{7/2}$ level of Nd^{3+} in the LaF_3 crystal for different values of the concentration. The curves were obtained by multiplying the luminescence decay kinetics by $\exp(t/\tau)$, where $\tau = 110.5$ ns, in order to exclude the intracenter nonradiative decay. The figure also shows model curves for $S = 6$ and 8, obtained by substituting the corresponding values of C_{DA} for the disordered stage into (11). The experimental and theoretical curves are superimposed in Fig. 5, assuming the disordered stage for $t > t_{\text{lim }1}$. The limiting time for transition from one type of decay to the other was calculated from the formula[12]

$$t_{\text{lim }1} = R_{min}^S/C_{DA} \qquad (12)$$

and was found to be 14.4, 2, and 0.32 ns for $S = 6$, 8, and 10, respectively. It is clear (Fig. 5) that the intial stage of nonradiative transfer is best described by the model curve (11) with $S = 6$. The discrepancy for $t < t_{\text{lim }1}$ and $S = 6$ is probably due to the fact that the laser pump pulse was not short enough. Its half-width for the curves with $c = 4.7$, 16.8, and 24.4% (Figs. 5a, c, and d) as approximately 8 ns; for $c = 11.3$% it was 15 ns (b). It is clear that latter case showed the highest initial discrepancy between the experimental and theoretical curves for $S = 6$. For the higher concentrations, and despite the fact that the rate of ordered decay was higher for them, the agreement between theory and experiment was better because the laser pulse length was shorter by a factor of about 2. For $c = 4.7$%, for which the rate of the ordered decay was the lowest and the pump pulse was short, the agreement between theory and experiment is excellent. For $S = 8$ and 10, there is a significant discrepancy between theory and experiment in the early stages of decay for all concentrations, and the discrepancy increases as a function of concentration.

Analysis of the results reproduced in Figs. 2–5 leads us to the conclusion that the transfer of energy from the $^4G_{7/2}$ excited state of the Nd^{3+} ion in the LaF_3 crystal occurs statically in accordance with the dipole-dipole mechanism

TABLE I. Values of the microparameter γ for nonradiative energy transfer from the $^4G_{7/2}$ level of Nd^{3+} in the LaF_3 crystal for different values of concentration and of the parameter S at 77 K.

n_A, 10^{20} cm^{-3}	c, %	γ, s$^{-3/S}$		
		$S=6$	$S=8$	$S=10$
8.3	4.7	3 478	593	233
19.8	11.3	8 432	1437	557
29.4	16.8	12 648	2055	801
42.8	24.4	18 069	3058	1096

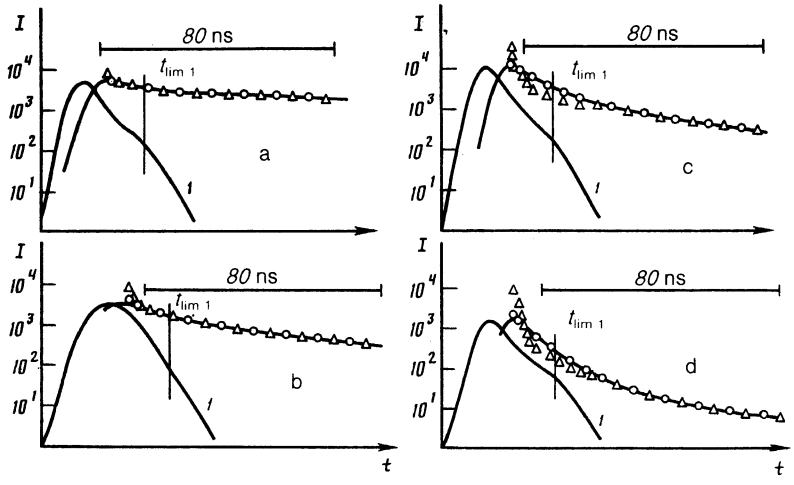

FIG. 5. Nonradiative energy transfer from the $^4G_{7/2}$ level of Nd^{3+} in the LaF_3 crystal at 77 K for different concentrations: (solid line—experimental, O—Kolubov and Konobeev, $S=6$ m, Δ—results for $S=8$) a—$c=4.7\%$, b—11.3%, c—16.8%, d—24.4%. Curve 1 is the instrumental function.

($S=6$) and a high value of the microparameter C_{DA}, i.e., 3.3×10^{-37} cm^6/s (which is greater than for the $^4F_{3/2}$ level).

In order to explain the strong concentration quenching of the $^4G_{7/2}$ state of the Nd^{3+} ion in the LaF_3 crystal, we use the Förster-Dexter theory of resonant multipolar interaction.[13] This assumes that the interaction probability W_{DA} in the donor-acceptor pair is proportional to the overlap integral of the donor luminescence spectrum and the acceptor absorption spectrum. The microparameter C_{DA} was estimated using the following formula that takes into account the Stark splitting of the multiplets of the rare earth ions in the crystal:

$$C_{DA}=\sum_{i'} n_{i'} \sum_{j} n_j \sum_{i} \sum_{j'} C_{DA_{jj'}}^{i'i}, \qquad (13)$$

where $n_{i'}$ is the population of the excited i'th level of Nd^{3+} (donor), n_j is the population of the unexcited jth level of Nd^{3+} (acceptor), and $C_{DA_{jj}}^{i'i}$ is given by

$$C_{DA_{jj'}}^{i'i}=\frac{9\chi^2 c\sigma_{D_{i'i}}\sigma_{A_{jj'}}\int F_{D_{i'i}}(\bar{\nu})F_{A_{jj'}}(\bar{\nu})\,d\bar{\nu}}{16\pi^4 n^2 \bar{\nu}_{max}^2}, \qquad (14)$$

where c is the velocity of light, $\bar{\nu}_{max}$ is the wave number at the maximum of the overlap spectrum (in cm^{-1}) whose area is normalized to the unit donor luminescence spectrum $F_{D_{i'i}}(\bar{\nu})$ and unit acceptor absorption spectrum $F_{A_{jj'}}(\bar{\nu})$, $\sigma_{D_{i'i}}$ and $\sigma_{A_{jj'}}$ are the corresponding integrated emission and absorption cross sections of donors and acceptors, respectively, n is the refractive index of the host ($n\approx1.6$ for LaF_3), and χ^2 represents the mutual orientation of dipoles in a pair of interacting particles. For immobile molecules (solid solutions), for which all the orientations of the dipole moments are equally probable, we can replace χ^2 with $0.84\times2/3$ (Ref. 13), although this averaging may not be entirely valid for Mg^{3+} ions which do not have a particular type of moment.

To identify the possible quenching and energy migration channels, we have measured the luminescence ($^4G_{7/2}\rightarrow{}^4I_{9/2}$; $^4I_{11/2}$; $^4I_{13/2}$ etc. transitions) and absorption ($^4I_{9/2}\rightarrow{}^4G_{7/2}$; $^2G_{7/2}+{}^4G_{5/2}$; $^4F_{9/2}$ etc. transitions) spectra corresponding to the highest frequency and strongest optical transitions in the Mb^{3+} ion in the LaF_3 crystal for $c=1\%$ and $T=77$ K. The reabsorption effect was minimized by reducing the optical density of the crystals. This did not produce any detectable change in the relative intensity of the luminescence spectral lines. As expected for the lanthanoid ion with weak electron-phonon coupling, the greatest overlap was observed for absorption and luminescence spectra resulting from the resonant $^4G_{7/2}\rightleftarrows{}^4I_{9/2}$ transition (see Fig. 6a). It was found that line maxima associated with identical inter-Stark transitions from levels populated at the given temperature were practically identical for the excited and ground states in both spectra.

The Förster theory of the two-body interaction was then used to analyze the migration microparameter C_{DD} ($W_{DD}=C_{DD}/R^6$) for the dipole-dipole interaction. In the case of the $^4G_{7/2}\rightleftarrows{}^4I_{9/2}$ resonant transition, the expression given by (14) can be substantially simplified, but account must be taken of the fact that the degeneracy ($g=2$) is the same for all the Stark sublevels of the Md^{3+} ion in the crystalline field of the LaF_3 lattice when degeneracy is completely lifted, which leads to equal emission and absorption cross sections ($\sigma_{i'i}=\sigma_{ii'}$) for a given transition. The luminescence line shape due to the $^4G_{7/2}(1')\rightarrow{}^4I_{9/2}(1)$ transition is reasonably well described by the Lorentz profile, which indicates that homogeneous broadening predominates over inhomogeneous broadening in ($\delta\gg\Delta$) for low concentrations of Md^{3+} ions in the LaF_3 crystal (the numbers in parentheses are the values of i' and j for Stark sublevels in multiplets).

For intermultiplet transitions between individual Stark levels with $i'>1$ and $j>1$, the above relationship between homogeneous and inhomogeneous broadening is satisfied with still greater precision because of the spontaneous emission of phonons that accompanies transitions between the Stark levels. Thus, by resolving the absorption spectrum due to the $^4I_{9/2}\rightarrow{}^4G_{7/2}$ transition into individual inter-Stark transitions, and assuming that the line shapes can be approximated by the homogeneous Lorentz profile, we obtain the following expression for the partial microefficiency of energy migration:

$$C_{DD}=n_{j'}9\chi^2 C\Gamma_{jj'}(k_{jj'})_{max}^2/64\pi^3 n^2(\bar{\nu}_{jj'})_{max}^2 N^2 n_j, \qquad (15)$$

where $\Gamma_{jj'}$ is the width of the homogeneous Lorentz profile describing the spectral line shape corresponding to the inter-Stark transition j–j', $(k_{jj'})_{max}$ is the absorption coefficient at

the maximum of the inter-Stark transition line, and $(\bar{\nu}_{jj'})_{max}$ is the wave number in cm^{-1} (at the maximum of the spectral line corresponding to the inter-Stark transition).

The value of C_{DD} calculated from (13) and (15) was found to be 1.6×10^{-39} cm^6/s, which is smaller by two orders of magnitude than the measured microparameter for quenching transfer. The value of C_{DD} that we have obtained enables us to define a model for possible migration energy quenching for the $^4G_{7/2}$ level of Nd^{3+} in the LaF_3 crystal on the basis of (4) and (5). In our case, $(C_{DA}/C_{DD})^{1/2}\approx10$, which suggests the diffusion model of migration quenching. For the sample with the lowest Mb^{3+} concentration that we have examined, $c = 24.4\%$ and the estimated migration probability was $\overline{W} = 2.5\times10^6$ s^{-1}. For $c = 16.8\%$, the calculated probability was $\overline{W} = 1.17\times10^6$ s^{-1}. Comparison of these quantities with the static decay rate $\gamma/t^{1/2}$ in our range of measured times shows that the correction introduced when migration was taken into account was small, and was certainly less than 6%.

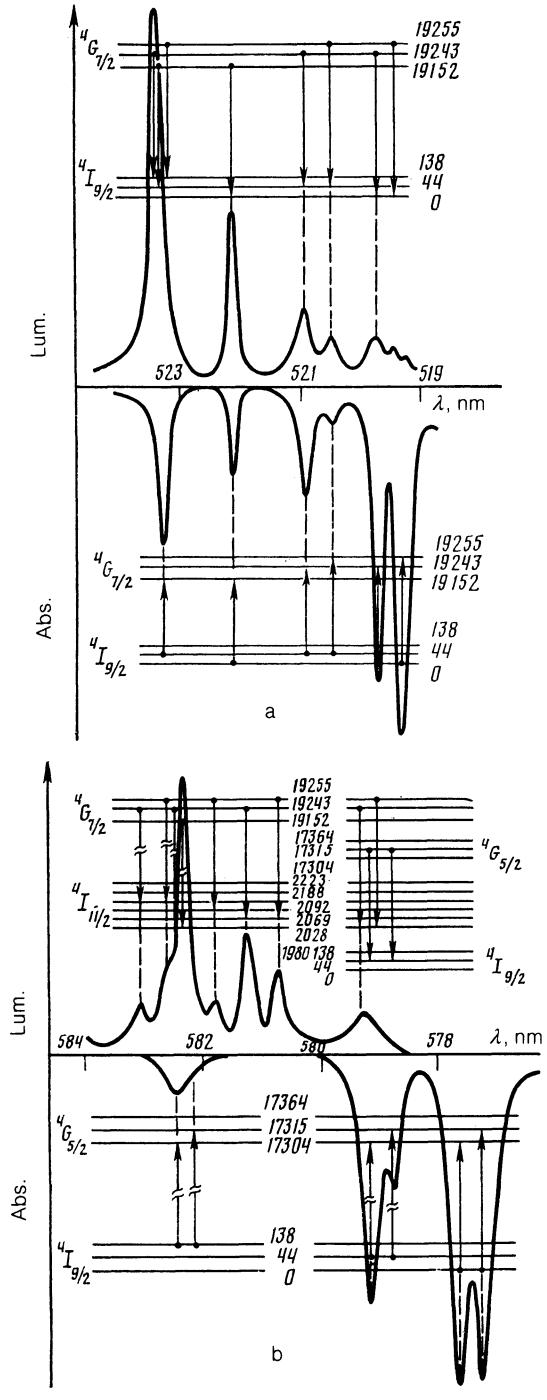

FIG. 6. Luminescence spectra for $\lambda_{exc} = 510.8$ nm and absorption spectra of Nd^{3+} in the LaF_3 crystal for the resonance transitions $^4G_{7/2}\rightarrow{}^4I_{9/2}$ and the $^4G_{7/2}\rightarrow{}^4I_{11/2}$ and $^4I_{9/2}\rightarrow{}^4G_{5/2}+{}^2G_{7/2}$ transitions (b) at $T = 77$ K and $c\leqslant1\%$).

A considerable overlap of absorption and emission spectra was also observed for the $^4I_{9/2}\rightarrow{}^4G_{5/2}+{}^2G_{7/2}$ and $^4G_{7/2}\rightarrow{}^4I_{11/2}$ transitions (see Fig. 6b). The energy transfer microefficiency C_{DA} was again calculated for this case from (13) but, instead of (14), we used the expression for the partial transfer microparameter $C^{i'i}_{DA_{jj'}}$ in terms of the spontaneous emission probability for different transitions (Einstein coefficients):

$$C^{i'i}_{DA_{jj'}} = \frac{9\chi^2 A_{i'i}\sigma_{jj'}\int F_{D_{i'i}}(\bar{\nu})F_{A_{jj'}}(\bar{\nu})\,d\nu}{4(2\pi)^5 n^4\bar{\nu}^4_{max}}, \qquad (16)$$

where $A_{i'i}$ is the probability of spontaneous emission as a result of the i'–i transition. The greatest difficulty in this method of determining the partial microparameters $C^{i'i}_{DA_{jj'}}$ was to find the probability of spontaneous emission $A_{i'i}$ in the region of overlap between donor luminescence and acceptor absorption spectra, since we have not been able to make direct measurements of the absorption spectrum due to the $^4I_{11/2}\rightarrow{}^4G_{7/2}$ transition because of the low population of the $^4I_{11/2}$ state. The spontaneous emission probability $A_{i'i}$ was therefore estimated from the ratio of the area under the luminescence spectrum due to the $^4G_{7/2}\rightarrow{}^4I_{11/2}$ transition in the region of the overlap and the area under the spectrum due to the resonant 1′–1 transition for which the cross section is known. The probability was calculated from the formula

$$A_{i'i}=A_{1'1}\frac{I_{i'i}}{I_{1'1}}\frac{(\nu_{1'1})_{max}}{(\bar{\nu}_{i'i})_{max}}\frac{n_{1'}}{n_{i'}}\frac{S(\bar{\nu}_{1'1})}{S(\bar{\nu}_{i'i})}, \qquad (17)$$

where $I_{i'i}$ and $I_{1'1}$ are the areas under the corresponding luminescence spectra, $A_{1'1}$ and $A_{i'i}$ are the spontaneous emission probabilities for the transitions $^4G_{7/2}(1')\rightarrow{}^4I_{9/2}(1)$ and $i'-1$, $(\bar{\nu}_{i'i})_{max}$ and $(\bar{\nu}_{1'1})_{max}$ are the wave numbers and the maxima of the emission lines produced in these transitions, and $S(\bar{\nu}_{1'1})/S(\bar{\nu}_{i'i})$ is the ratio of the measured spectral sensitivities of the photomultiplier at the wavelengths corresponding to the excited Stark levels. The probability $A_{1'1}$ of the $1'-1$ transition was found from the corresponding absorption spectrum for the $1-1'$ transition, using the formula[15]

$$A_{1'1}=\frac{8\pi c(\bar{\nu}_{1'1})^2_{max}}{n_A n_1 n}\int k_{11'}(\bar{\nu})\,d\bar{\nu}. \qquad (18)$$

In this procedure, the luminescence spectrum due to the $^4G_{7/2}\rightarrow{}^4I_{11/2}$ transition was first resolved into the individual inter-Stark components. A complete resolution (either in wavelength or in time) could not be achieved near $\lambda = 579$ nm (Fig. 6b) for the luminescence emitted as a result of the $^4G_{7/2}\rightarrow{}^4I_{11/2}$ and $^4G_{5/2}+{}^2G_{7/2}\rightarrow{}^4I_{9/2}$ transitions under excitation to the $^4G_{7/2}$ level. To estimate the upper limit, we assumed that the luminescence emitted from the mixed mul-

tiplet $^4G_{5/2} + {}^2G_{7/2}$ was absent from the spectrum and that the entire luminescence band near $\lambda = 579$ nm was due to the $^4G_{7/2} \rightarrow {}^4I_{11/2}$ transition. In Fig. 6b, the double cross-bars mark transitions providing the main contribution to the overlap integral in the visible range. The microparameter C_{DA} was determined by a numerical technique whereby the trapezoid method was used to evaluate the overlap integral for two regions in the absorption spectrum due to the $^4I_{9/2} \rightarrow {}^4G_{5/2} + {}^2G_{7/2}$ transition, namely, $\lambda_1 = 579$ nm and $\lambda_2 = 582$ nm (because, in each of these, absorption occurs only from the single Stark multiplet $^4I_{9/2}$—from the second to the first and from the third to the second) with each of the inter-Stark spectral lines due to the overlapping $^4G_{7/2} \rightarrow {}^4I_{11/2}$ transition. The overlap integrals obtained in this way were substituted in (16), and the resulting partial values of the microparameter were summed with allowance for their relative importance, depending on the population of their Stark components according to (13). The transfer microparameter determined in this way was found to be 1.7×10^{-40} cm^6/s, which is higher by almost an order of magnitude than for the metastable $^4F_{3/2}$ level, but is lower by three orders of magnitude than the measured value.

We have thus established an anomalously large difference ($> 10^3$) between the experimental transfer microparameter C_{DA} and the value calculated from the overlap integral using the Förster resonance theory for the $^4G_{7/2}$ level of the Nd^{3+} ion in LaF_3 crystal.

To elucidate the mechanism and nature of the anomalously high quenching of the $^4G_{7/2}$ level of the Nd^{3+} ion in the LaF_3 crystal, we have examined experimentally the kinetics of luminescence decay for levels lying above and below the level under investigation, i.e., the $^4G_{5/2} + {}^2G_{7/2}$, $^2P_{3/2}$ and $^4D_{3/2}$ levels.[16]

The luminescence decay kinetics was measured in the case of the $^4G_{5/2} + {}^2G_{7/2}$ transition of Nd^{3+} in the range 0–100 ns, with the intensity varying by three orders of magnitude for $c = 24.4\%$ and $T = 77$ K. It was found that the luminescence decayed almost exponentially with a characteristic time constant $\tau = 12.2$ ns, which is lower by a factor of approximately two as compared with $c = 1\%$ (Ref. 5). The value of C_{DA} calculated for the ordered stage using (7) was found to be 7.7×10^{-38} cm^6/s. The limiting time of transition to the disordered stage, calculated from (12), was found to be $t_{\lim 1} = 66$ ns. If we assume that the total number of donors radiating on the ordered stage can be estimated very approximately from the formula[17]

$$I_y = 1 - \exp(-W_0 t_{\lim 1}), \qquad (19)$$

we find that the result is approximately 95%. We therefore conclude that we observed the entire ordered stage of decay, but only the initial part of the disordered stage. If we estimate the energy migration microparameter for the resonant transition $^4G_{5/2} + {}^2G_{7/2} \rightarrow {}^4I_{9/2}$ at $T = 77$ K, using the Förster resonance theory, i.e., (13) and (14), we find $C_{DD} = 6.0 \times 10^{-39}$ cm^6/s, which is lower by a factor of 13 than the value deduced from kinetic measurements for this level.

By using a tunable picosecond dye laser with a pulse repetition frequency of 10 ns (Ref. 16) to pump the $^4G_{5/2} + {}^2G_{7/2}$ level of Nd^{3+}, we were able to measure the exponential decay corresponding to the ordered stage of nonradiative transfer. The value of C_{DA} was found to be $(1.2 \pm 0.2) \times 10^{-37}$ cm^6/s at $T = 300$ K, which is higher by a factor of 1.5 than the result for $T = 77$ K. This suggests a change in the sign of the temperature dependence of C_{DA} for the $^4G_{5/2} + {}^2G_{7/2}$ level as compared with the $^4G_{7/2}$ level. The limiting time of transition to the disordered stage at $T = 300$ K, calculated from (12), is $t_{\lim 1} = 45$ ns. Analysis of the luminescence and absorption spectra enabled us to find the overlap between the luminescence spectra due to the $^4G_{5/2} + {}^2G_{7/2} \rightarrow {}^4I_{13/2}$ transitions from the excited state and the absorption spectra ($^4I_{9/2} \rightarrow {}^4F_{7/2} + {}^4S_{3/2}$ transitions) from the ground state which indicated the possible presence of a crossrelaxation quenching channel.

The decay of luminescence emitted as a result of transitions from the $^4D_{3/2}$ level of Nd^{3+} in LaF_3 was measured for $c = 1$ and 2.5% at $T = 300$ K (Fig. 7) under third-harmonic excitation by a Nd:YAG laser pumped by a continuously-operating gas-filled lamp, using passive Q-switching by a LiF:F_2^- crystal. For $c = 1\%$ (curve 1), the decay was exponential with a lifetime $\tau = 13.5$ μs, but was more rapid and nonexponential for $c = 2.5\%$ (curve 2).

When the transfer microparameter C_{DA} was estimated for the $^4D_{3/2}$ level for $c = 2.5\%$ and $T = 300$ K, using the Goludov-Konobeev expression (11), we found $C_{DA} = 0.84 \times 10^{-38}$ cm^6/s. This is almost 20 times lower than the quenching efficiency for the $^4G_{7/2}$ level, but greater by a factor of 280 than the value of C_{DA} for the $^4F_{3/2}$ level. We can thus see that, at $T = 300$ K, the microefficiency of the quenching energy transfer from the $^4D_{3/2}$ level, which lies above the $^4G_{7/2}$ state on the energy scale, is substantially lower in magnitude. This suggests the absence of quenching mechanisms associated with high-lying charge-transfer levels and excitonic or band states that could be responsible for the anomalously strong quenching of luminescence due to high-lying levels of Nd^{3+}.

Such a large difference between the values of the measured and calculated (from Förster's theory) energy-transfer microparameters may be due to a possible increase in the emission probability in transitions participating in the above cross relaxation (and the corresponding increase in the quenching microefficiency C_{DA}) as the Nd–Nd inter-ionic separation is reduced with increasing impurity concentration. However, the concentration dependence of the area under the absorption spectrum was found to be linear for each of the transitions to the different high-lying levels $^4G_{9/2}$, $^4G_{7/2}$, $^4G_{5/2}$, $^2G_{7/2}$ and $^4S_{3/2}$ from the ground state $^4I_{9/2}$ of the Nd^{3+} ion in the LaF_3 crystal at $T = 300$ K.

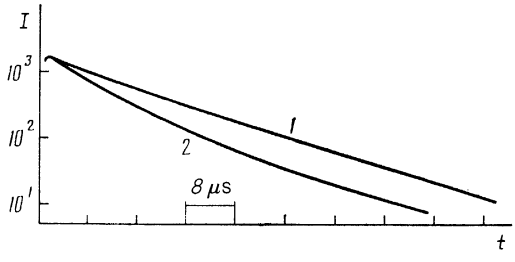

FIG. 7. Decay of luminescence from the $^4D_{3/2}$ level of Nd^{3+} at 300 K in the LaF_3 crystal for different concentrations ($\lambda_{exc} = 355$ nm, $\lambda_{reg} = 362.5$ nm): 1—$c = 1\%$, 2—$c = 2.5\%$.

To verify the validity of the proposed channel for the quenching of the $^4G_{7/2}$ level of Nd^{3+} in the LaF_3 crystal via the $^4G_{5/2} + {}^2G_{7/2}$ level, we have examined the luminescence spectra in range $\lambda = 588$–596 nm (Fig. 8) for crystals with different concentration (curve 2—$c = 1\%$, curve 3—4.7%, and curve 4—24.4%) under excitation to the $^4G_{7/2}$ state. The spectral lines were identified by comparing the luminescence spectra for $c = 4.7\%$ in the above range under excitation to the $^4G_{7/2}$ level (curve 3) and the $^4G_{5/2} + {}^2G_{7/2}$ (curve 1) levels. This comparison, and the analysis of inter-Stark splitting of the levels of Nd^{3+} in the LaF_3 crystal,[18] showed that peak A corresponds to the $(^4G_{5/2} + {}^2G_{7/2})(1) \rightarrow {}^4I_{9/2}(5,6)$ transition, whereas peaks B and C correspond to the $^4G_{7/2}(1) \rightarrow {}^4I_{11/2}(5)$, $^4I_{11/4}(6)$ transitions, respectively.

Analysis of the luminescence spectra for $c = 24.4\%$ shows that peak A broadens and its maximum shifts toward lower frequencies (see Fig. 8, curves 2 and 4), suggesting that there is a change in the parameters of the internal crystal field acting on the Nd^{3+} ions, which in turn leads to an increase in the inhomogeneous broadening as a consequence of the disordering of the structure of the crystal. The luminescence lines B and C of the above $^4G_{7/2} \rightarrow {}^4I_{11/2}$ inter-Stark transitions vanish almost completely for $c = 24.4\%$. This change in the spectra with increasing concentration can be explained by examining possible intra- and intercenter transitions in a pair of ions (excited and unexcited). For excitation to the $^4G_{7/2}$ level, radiationless deactivation consist of two processes, namely, relaxation inside the center, which populates the lower-lying multiplet $^4G_{5/2} + {}^2G_{7/2}$, and energy transfer between centers (Nd–Nd), which can proceed to the latter multiplet or to some other lower-lying one. The intracenter probability W_{RR} of radiationless relaxation from the $^4G_{7/2}$ level is lower for $c = 24.4\%$ than the probability of radiationless energy transfer $W_F = \gamma^2$ by a factor of almost 55. This means that, when there is no energy transfer to the lower-lying multiplet $^4G_{5/2} + {}^2G_{7/2}$, its population by radiationless multiphonon relaxation during excitation to the $^4G_{7/2}$ state will occur with very low efficiency ($\eta = W_{RR}/W_F \approx 0.02$). If we also take into account the intrinsic and relatively strong concentration quenching of the $^4G_{5/2} + {}^2G_{7/2}$ state, which is weaker by a factor of only 4.7 than the quenching of the $^4G_{7/2}$ state, the peak A due to luminescence from the $^4G_{5/2} + {}^2G_{7/2}$ should not appear in the spectrum. No strong luminescence peak due to the above inter-Stark transition (peak A) is in fact observed. It seems to us that this is a strong indication that nonradiative energy transfer from the $^4G_{7/2}$ level proceeds to the $^4G_{5/2} + {}^2G_{7/2}$ state.

Figure 9 shows the probability of intracenter nonradiative multiphonon relaxation, W_{RR}, for a number of excited

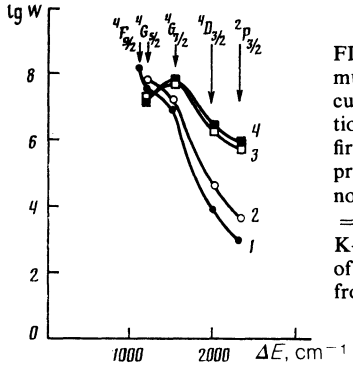

FIG. 9. Probability of nonradiative multiphoton relaxation (77 K—curve 1, 300 K—curve 2) as a function of the energy gap ΔE_{min} to the first lower-lying multiplet and the probability of intercenter Nd–Nd nonradiative transfer $W^0_{DA} = C_{DA}/R^6_{min}$ (77 K—curve 3, 300 K—curve 4) from high-lying levels of Nd^{3+} in the LaF_3 crystal (data from Refs. 5, 16, and 24).

states of the Nd^{3+} ion in the LaF_3 crystal. It was determined from the luminescence decay data for these levels under direct or laser excitation for different values of the energy gap ΔE_{min} to the nearest lower-lying multiplet and two values of temperature, namely, $T = 77$ and 300 K (curves 1 and 2), and also the probability of intercenter nonradiative energy transfer from these levels for the minimal separations between the ions ($W^0_{DA} = C_{DA}/R^6_{min}$) at the same temperatures (curves 3 and 4). When W_{RR} was determined for each of the excited levels, we subtracted the probability A of spontaneous decay for the reciprocal of the lifetime $W_{RR} = 1/\tau_m - A$, where A was determined from the Judd-Ofelt theory, using the data reported in Refs. 19–22. The probability A of radiative transitions for the $^4G_{7/2}$ and $^4G_{5/2} + {}^2G_{7/2}$ levels is $\sim 0.01\%$ of the corresponding nonradiative probability W_{RR} ($A \ll W_{RR}$). The relation $W_{RR} = 1/\tau_m$ is therefore satisfied with high precision. For the $^4D_{3/2}$ and $^2P_{3/2}$ levels, the radiative transition probability A lies in the range 15–70% of W_{RR}. Accordingly, the precision with which W_{RR} is determined for these levels is lower because of the approximate nature of the Judd-Ofelt theory. It is clear (Fig. 9) that for values of the energy gap greater than 1500 cm^{-1}, i.e., for the $^4G_{7/2}$, $^4G_{3/2}$, and $^2P_{3/2}$ multiplets, there is a correlation between the dependence of the nonradiative energy transfer and the nonradiative multiphonon relaxation probabilities on the energy gap ΔE_{min}.

The last fact, and also the considerable discrepancy between the measured and calculated (from the overlap integral) values of the microparameter C_{DA} deduced from the donor luminescence spectrum ($^4G_{7/2} \rightarrow {}^4I_{11/2}$) and the acceptor absorption spectrum ($^4I_{9/2} \rightarrow {}^4G_{5/2} + {}^2G_{7/2}$), using the Förster theory for the $^4G_{7/2}$ level, suggests to us that energy transfer from the excited states of the Nd^{3+} ion in the LaF_3 crystal is governed by a nonresonant multiphonon mechanism. It is shown in Ref. 23 that, when the optical

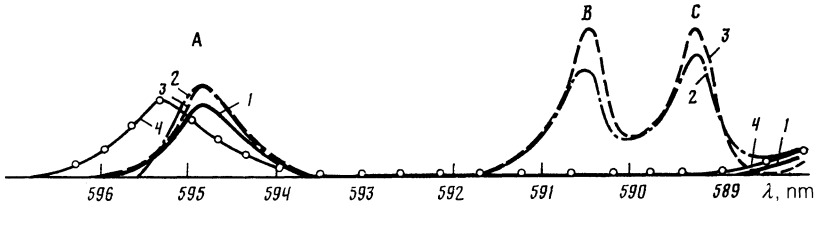

FIG. 8. Luminescence due to the $(^4G_{5/2} + {}^2G_{7/2})(1) \rightarrow {}^4I_{9/2}(5)$ transitions for $\lambda_{exc} = 578.2$ nm and $c = 4.7\%$—curve 1; $(^4G_{5/2} + {}^2G_{7/2})(1) \rightarrow {}^4I_{9/2}(5.6)$—(A) and $^4G_{7/2}(1) \rightarrow {}^4I_{11/2}(5.6)$—(B) and (C) for $\lambda_{exc} = 510.8$ nm, $c = 1\%$—curve 2, $c = 4.7\%$—curve 3, $c = 24.4\%$—curve 4.

center is weakly coupled to the crystal field (RE in a solid), the relative contribution of the N-phonon process to the transition probability in the case of energy transfer is greater than the probability of nonradiative relaxation by the factor $(1+g_A/g_D)^N$, where g_D and g_A are the donor and acceptor electron-phonon coupling strengths, respectively. The reduction in the probability of multiphonon energy transfer with increasing energy gap $\Delta E_{\min}$ (and with the ratio $N=\Delta E_{\min}/\hbar\omega_{\Phi\Phi}$) should occur more slowly than the reduction in the probability of multiphonon nonradiative relaxation.

The above dependence of the probabilities on the energy gap is confirmed by Fig. 9 for $\Delta E_{\min} > 1500\ \text{cm}^{-1}$. We can therefore try to use the functions $W^0_{DA}(N)$ and $W_{RR}(N)$ to determine the coupling strengths for the donor and acceptor transitions of the Nd^{3+} ion (g_A/g_D). The values obtained, $g_A/g_D = 1.8$–44.1, show that there is a considerable variation (by more than an order of magnitude), suggesting that this model is in poor agreement with experimental data. Moreover, there are additional facts that contradict the nonresonant multiphonon nature of the Nd–Nd energy transfer from high-lying levels. They include, first, the lack of correlation between W^0_{DA} and W_{RR} for $\Delta E < 1500\ \text{cm}^{-1}$. In particular, when $\Delta E_{\min} = 1200\ \text{cm}^{-1}$ and $T = 77$ K, the transfer probability is lower as compared with $\Delta E_{\min} = 1546\ \text{cm}^{-1}$, whereas the probability of nonradiative multiphonon relaxation is found to increase. Second, as T rises from 77 to 300 K, the probability of intracenter multiphonon relaxation increases for all the levels that we have examined. This is due to the increase in the population of phonon modes with high energies as the temperature increases, and is actually observed only for the $^4G_{5/2}+{}^2G_{7/2}$ level. For all the other levels, there is a reduction in the transfer probability when the temperature is raised from 77 to 300 K.

It must therefore be admitted that, although there is a measure of agreement between the energy transfer probability as a function of the energy gap $\Delta E_{\min}$ to the nearest lower-lying multiplet and its behavior in the case of nonresonant multiphonon transfer, there are also several differences that are incompatible with the above mechanism.

The result is that neither the resonant crosscorrelational scheme ($^4G_{7/2}\rightarrow{}^4I_{11/2}$, $^4I_{9/2}\rightarrow{}^4G_{5/2}+{}^2G_{7/2}$) nor the nonresonant multiphonon mechanism ($^4G_{7/2}\rightarrow{}^4I_{9/2}+x\hbar\omega_{\max}$, $^4I_{9/2}\rightarrow{}^4G_{5/2}+(N-x)\hbar\omega_{\max}$) can be the main mechanism responsible for the concentration quenching of the $^4G_{7/2}$ levels of Nd^{3+} in the LaF_3 crystal. However, we have shown that energy transfer does occur from this level to the first lower-lying multiplet $^4G_{5/2}+{}^2G_{7/2}$. This means that we are left with the last crossrelaxational quenching channel that we have not as yet examined, namely, that involving transitions to the infrared ($\lambda\sim 5\ \mu$m): $^4G_{7/2}\rightarrow{}^4G_{5/2}+{}^2G_{7/2}$, $^4I_{9/2}\rightarrow{}^4I_{11/2}$. Moreover, whilst the second of these transitions is readily observed in the infrared absorption spectrum, the infrared luminescence spectrum due to the $^4G_{7/2}\rightarrow{}^4G_{5/2}+{}^2G_{7/2}$ transition from a highly-quenched level is exceedingly difficult to detect, and the Stark splitting of the $^4G_{7/2}$ and $^4G_{5/2}+{}^2G_{7/2}$ levels can only yield the spectrum range occupied by this luminescence.

Estimates based on the Judd-Ofelt theory show that the probability A of $^4G_{7/2}\rightarrow{}^4G_{5/2}+{}^2G_{7/2}$ spontaneous emission is lower by a factor by almost 400 as compared with the $^4G_{7/2}\rightarrow{}^4I_{11/2}$ transition, and the absorption cross section σ_A for the $^4I_{9/2}\rightarrow{}^4I_{11/2}$ transition is lower by a factor of nearly five as compared with the $^4I_{9/2}\rightarrow{}^4G_{5/2}+{}^2G_{7/2}$ transition. However, despite this, and if we turn to (16), we see that the energy transfer microparameter C_{DA} depends significantly not only on A and σ_A, but also on the frequency of transitions participating in the crosscorrelation process. In particular, the microparameter C_{DA} is inversely proportional to the fourth power of the wave number at the maximum of the overlap integral. Physically, this is due to the fact that the probability of energy transfer from a donor to an acceptor is proportional to the overlap integral multiplied by the squares of the matrix elements of the dipole-dipole transitions in the donor and acceptor[13]:

$$W_{DA} \propto |\hat{H}_D|^2 |\hat{H}_A^2| \int F_D(\bar{\nu}) F_A(\bar{\nu})\, d\bar{\nu}.$$

The product of these squares of matrix elements, estimated from the Judd-Ofelt theory for the $^4G_{7/2}\rightarrow{}^4G_{5/2}+{}^2G_{7/2}$, $^4I_{9/2}\rightarrow{}^4I_{11/2}$ transitions in the infrared, is greater by a factor of nearly five than the analogous product for the $^4G_{7/2}\rightarrow{}^4I_{11/2}$, $^4I_{9/2}\rightarrow{}^4G_{5/2}+{}^2G_{7/2}$ transitions in the visible, although the product of A and σ_A shows the reverse behavior because of the strong frequency dependence $A_D\propto\bar{\nu}^3$ and $\sigma_A\propto\bar{\nu}$. Moreover, analysis of the Stark structure of levels participating in these processes, shows that the overlap between the donor luminescence and acceptor absorption spectra in the case of the crossrelaxational infrared channel is much greater than in the visible range. All this suggests that quenching according to the cross-relaxational scheme $^4G_{7/2}\rightarrow{}^4G_{5/2}+{}^2G_{7/2}$, $^4I_{9/2}\rightarrow{}^4I_{11/2}$ can occur more effectively by 1–3 orders of magnitude than in the $^4G_{7/2}\rightarrow{}^4I_{11/2}$, $^4I_{9/2}\rightarrow{}^4G_{5/2}+{}^2G_{7/2}$ channel. These rates are close to values obtained experimentally from measurements of decay kinetics.

Figure 10 shows the $^4I_{9/2}\rightarrow{}^4I_{11/2}$ absorption spectrum of the Nd^{3+} ion in the LaF_3 crystal, as recorded by the IKS-20 infrared spectrometer (Fig. 10a), together with the luminescence spectral range deduced from the proposed energy scheme for luminescence between the levels under investigation and the nearest lower-lying multiplets, taking into account the thermal population of the Stark sublevels at $T = 77$ K and 300 K. It is clear that the maximum overlap with the spectrum occurs for the $^4G_{7/2}\rightarrow{}^4G_{5/2}+{}^2G_{7/2}$ transition. The overlap occurs at the maxima of the absorption spectra for both 77 and 300 K. We know that an increase in temperature is accompanied by an increase in the homogeneous widths of spectral lines due to inter-Stark transitions and in the total width of the band of intermultiplet transitions due to the population of higher-lying Stark sublevels. For luminescence and absorption lines that are in exact resonance ($\bar{\nu}^{\text{lum}}_{\max}=\bar{\nu}^{\text{abs}}_{\max}$), temperature broadening will lead to a reduction in the overlap integral and, hence, to a reduction in C_{DA}.

We therefore conclude that, as the temperature increases, the magnitude of C_{DA} should decrease for the $^4G_{7/2}$ level, but the reduction should be very small because the broadening is small. This is in good agreement with our experimental data in Fig. 9. Analysis of Figs. 9 and 10 shows that a very similar situation occurs for the $^4D_{3/2}$ level, although the probability A of the spin-forbidden $^4D_{3/2}\rightarrow{}^2P_{3/2}$ transition and the overlap of the donor and acceptor spectra

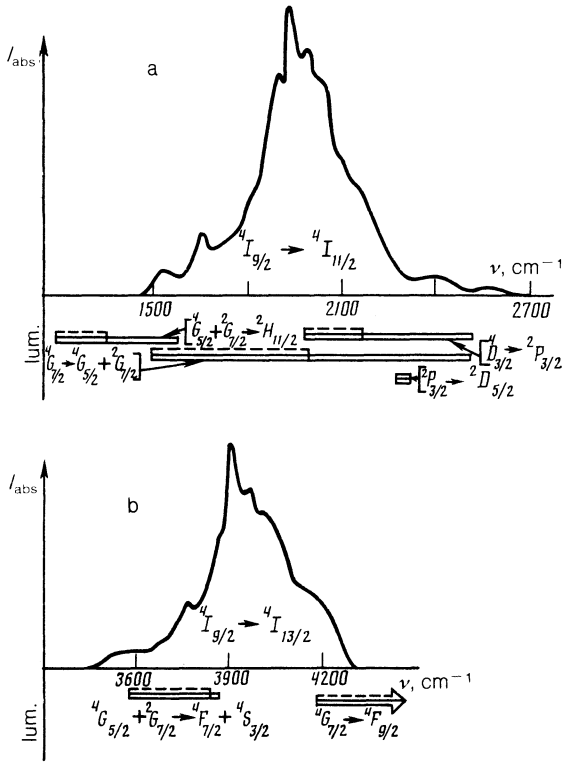

FIG. 10. Analysis of quenching relaxational interactions (Nd^{*3+}–Nd^{3+}) in the LaF_3 crystal. The figure shows the possible overlap of luminescence spectra from different high-lying levels of Nd^{3+} together with the absorption spectrum: *a*—$^4I_{9/2} \rightarrow {}^4I_{11/2}$, b—$^4I_{9/2} \rightarrow {}^4I_{13/2}$ transition at 77 K—dashed line, and at 300 K—solid line.

should now be smaller than for the $^4G_{7/2}$ level with the same sign of the temperature dependence. For the $^2P_{3/2}$ level, the possible overlap of donor and acceptor spectra is also very small. The magnitude of C_{DA} is therefore found to be small.

The reverse situation occurs for the $^4G_{5/2} + {}^2G_{7/2}$ level for which the theoretically possible overlap between luminescence and absorption spectra at $T = 300$ K is much greater than at 77 K. The measured C_{DA} for this level at 300 K is actually also greater than for 77 K.

We must therefore conclude that we have to take into account the possibility of overlap between the infrared luminescence spectra associated with these multiplets and the $^4I_{9/2} \rightarrow {}^4I_{13/2}$ absorption spectrum in the spectral range $\lambda \sim 2.5\ \mu$m (Fig. 10b). The square of the matrix element of the $^4I_{9/2} \rightarrow {}^4I_{13/2}$ acceptor transition, determined from the absorption spectra, is smaller by a factor of only 4 than for the $^4I_{9/2} \rightarrow {}^4I_{11/2}$ transition. Moreover, according to the Judd-Ofelt theory, the square of the matrix element, e.g., of the $^4G_{7/2} \rightarrow {}^4F_{9/2}$ donor transition, is smaller by a factor of only 2.7 than for the $^4G_{7/2} \rightarrow {}^4G_{5/2} + {}^2G_{7/2}$ transition. However, it is clear from Fig. 10b that the possible range of the $^4G_{7/2} \rightarrow {}^4F_{9/2}$ luminescence overlaps the absorption spectrum only at the very edge. Luminescence from the $^4D_{3/2}$ and $^2P_{3/2}$ levels should not overlap the $^4I_{9/2} \rightarrow {}^4I_{13/2}$ absorption spectrum at all. The opposite situation prevails for the $^4G_{5/2} + {}^2G_{7/2}$ level because the possible range of the $^4G_{5/2} + {}^2G_{7/2} \rightarrow {}^4F_{7/2} + {}^4S_{3/2}$ luminescence spectrum is found practically to overlap the maximum of the above absorption spectrum. All this shows that, first, $^4G_{5/2} + {}^2G_{7/2}$ quenching can occur via both the infrared crossrelaxational quenching channels, and, second, the $^4G_{5/2} + {}^2G_{7/2}$ level is quenched to a greater extent in the second channel at 300 K than at 77 K.

We therefore conclude that we have measured, for the first time, the two-stage kinetics of quenching nonradiative energy transfer in the case of the excited states of rare-earth ions in the nanosecond range. All the measured and calculated transfer and energy migration microparameters (C_{DA} and C_{DD}) are in good agreement with the Förster resonance theory for a number of excited high-lying levels of Nd^{3+} in the LaF_3 crystal. The main contribution to the resultant microparameter C_{DA} for transfer from high-lying $^4G_{7/2}$ and $^4G_{5/2} + {}^2G_{7/2}$ levels is provided by the lowest-frequency crossrelaxational transitions in the infrared.

The authors are indebted to S. Kh. Batygov and the staff of the Division of Solid State Physics of the Institute of General Physics of the USSR Academy of Sciences for providing them with the crystals, V. A. Myzina for measuring the concentration of Nd^{3+} ions in the LaF_3 crystal with the Camebax system, A. Yu. Dergachev for the $\lambda = 354$ nm laser with a high pulse repetition frequency for the excitation of the $^4D_{3/2}$ level, B. O. Orlovskaya for assistance in producing this text, and the staff of the Bucharest Central Institute of Physics, including Sch. Dzhordzhesku, A. Lupeĭ and V. Lupeĭ for fruitful discussions of our results.

[1]R. M. Macfarlane, F. Tong, and W. Length, 16th Intern. Conf. on Quant. Electron (IQEC'88), Tech. digest, p. 570, Tokyo, 1988.
[2]Yu.K. Voron'ko, T. G. Mamedor, V. V. Osiko *et al.*, Zh. Eksp. Teor. Fiz. **71**, 478 (1976) [Sov. Phys. JETP **44**, 252 (1976)].
[3]R. Buisson and Q. Liu, J. Phys. (Paris) **45**, 1523 (1984).
[4]O. K. Alimov, M. Kh. Ashurov, T. T. Basiev, *et al.*, Trudy IOFAN **9**, 50 (1987).
[5]T. T. Basiev, A. Yu. Dergachev, E. O. Kirpichenkova, Kvantovaya Elektron. (Moscow) **14**, 2021 (1987) [Sov. J. **14**, 1281 (1987)].
[6]I. A. Bondar', A. I. Burshtein, A. V. Krutikov, *et al.*, Zh. Eksp. Teor. Fiz. **81**, 96 (1981) [Sov. Phys. JETP **54**, 45 (1981)].
[7]M. Yokota and O. Tanimoto, J. Phys. Soc. Jpn. **22**, 779 (1967).
[8]A. I. Burshtein, Zh. Eksp. Teor. Fiz. **62**, 1695 (1972) [Sov. Phys. JETP **35**, 882 (1972)].
[9]Th. Forster, Z. Naturforsch. A **B4**, 321 (1949); M. Ynokuti and F. Hirayama, J. Chem. Phys. **43**, 1978 (1965).
[10]S. I. Golubov and D. V. Konobeev, Fiz. Tverd. Tela (Leningrad) **13**, 3185 (1971) [Sov. Phys. Solid State **13**, 2679 (1971)].
[11]I. Oftedal, Z. Phys. Chem. **B5**, 272 (1929); W. M. Mansmann, Z. Kristall. **122**, 375 (1965).
[12]V. P. Sakun, Fiz. Tverd. Tela (Leningrad) **14**, 2199 (1972) [Sov. Phys. Solid State **14**, 1906 (1972)].
[13]D. L. Dexter, J. Chem. Phys. **21**, 836 (1953).
[14]M. D. Galanin, Zh. Eksp. Teor. Fiz. **28**, 485 (1955) [Sov. Phys. JETP **1**, 317 (1955)].
[15]G. F. Imbush and R. Kopelman, *Laser Spectroscopy of Solids*, eds. W. M. Yen and P.M. Sleser, Springer-Verlag, N.Y., 1981, p. 1.
[16]T. T. Basiev and Yu. A. Dergachev, and Yu. V. Orlovskiĭ, *et al.*, Tunable Solid State Lasers Conference, North Falmouth, USA, Techn. Digest, p. 171, 1981.
[17]A. G. Avanesov, T. T. Basiev, Yu. K. Voron'ko *et al.*, Zh. Eksp. Teor. Fiz. **84**, 1028 (1983) [Sov. Phys. JETP **57**, 596 (1983)].
[18]A. A. Kaminskiĭ, *Laser Crystals*, Springer, New York (1981).
[19]W. T. Carnal, P. R. Fields, and K. Rajnak, J. Chem. Phys. **49**, 4424 (1968).
[20]W. F. Krupke, Phys. Rev. **145**, 325 (1966).
[21]W. F. Krupke, IEEE J. Quant. Electron. **7**, 153 (1977).
[22]E. B. Sveshnikova, A. A. Stroganov, *et al.*, Opt. Spektrosk. **63**, 1047 (1987) [Opt. Spectrosc. (USSR) **63**, 618 (1987)].
[23]T. Miyakawa and D. L. Dexter, Phys. Rev. **B1**, 2961 (1970).
[24]T. T. Basiev, Yu. A. Dergachev, and Yu. V. Orlovskiĭ, 3rd Intern. Conf. Trends in Quant. Electron, eds. I. Ursu and A. M. Prokhorov, Eur. Phys. Soc. Abstracts, p. 100, 1988.

Translated by S. Chomet